Triboluminescence of alkaline earth aluminate polycrystals doped with Dy^{3+}

Katsuhisa Tanaka[a)]
Department of Chemistry and Materials Technology, Faculty of Engineering and Design, Kyoto Institute of Technology, Matsugasaki, Sakyo-ku, Kyoto 606-8585, Japan

Koji Fujita, Tomohiro Taniguchi, and Kazuyuki Hirao
Department of Material Chemistry, Graduate School of Engineering, Kyoto University, Yoshidahonmachi, Sakyo-ku, Kyoto 606-8501, Japan

Tsuguo Ishihara
Hyogo Prefectural Institute of Industrial Research, 3-1-12, Suma-ku, Kobe 654-0037, Japan

(Received 24 April 2000; accepted for publication 10 July 2000)

Triboluminescence spectra have been measured for polycrystalline $(Sr,Ba)Al_2O_4$ and $(Sr,Ca)Al_2O_4$ doped with Dy^{3+}. $Sr_{1-x}Ba_xAl_2O_4:Dy^{3+}$ with $x=0$, 0.1, 0.2, and 0.4 and $Sr_{0.9}Ca_{0.1}Al_2O_4:Dy^{3+}$ clearly exhibit triboluminescence caused by the $4f-4f$ transitions of Dy^{3+}. In contrast, triboluminescence is barely observed in $Sr_{0.8}Ca_{0.2}Al_2O_4:Dy^{3+}$ and $Sr_{0.6}Ca_{0.4}Al_2O_4:Dy^{3+}$ although both of them show photoluminescence due to the $4f-4f$ transitions of Dy^{3+}. For the $Sr_{1-x}Ba_xAl_2O_4:Dy^{3+}$ with $x=0$, 0.1, 0.2, and 0.4 and $Sr_{0.9}Ca_{0.1}Al_2O_4:Dy^{3+}$, the compositional dependence of the relative integrated intensity of the emission lines is different between triboluminescence and photoluminescence spectra. We suggest two possibilities to explain this phenomenon; one of them is the self-absorption by Dy^{3+} in the case of triboluminescence, and the other is a situation that a strain is imposed on Dy^{3+}, which brings about the triboluminescence due to the $4f-4f$ transitions. We speculate that the latter is the main cause for the difference between triboluminescence and photoluminescence spectra. © *2000 American Institute of Physics.* [S0021-8979(00)03020-6]

I. INTRODUCTION

Rare-earth-containing inorganic solids including crystals and glasses exhibit very interesting optical properties peculiar to the electronic states and transitions among them of each of the rare-earth ions. The optical properties of those solids are important for fabrication of optoelectronics devices such as a laser, an optical amplifier, an optical memory, a magneto-optical device, and so forth. Some inorganic crystals doped with rare-earth ions exhibit triboluminescence with various colors characterized by the electronic transitions of the rare-earth ions. The triboluminescence is a phenomenon that a solid emits photons when it is fractured or deformed.[1] This phenomenon has been observed in many kinds of solids including ionic crystals, semiconductors, metals, minerals, glasses, and organic crystals.[2–13] Chapman and Walton[14] demonstrated that CaF_2 single crystals doped with trivalent rare-earth ions show triboluminescence ascribable to the electronic transitions of the doped rare-earth ions. Ishihara and co-workers[15,16] revealed that polycrystalline barium hexacelsians ($BaAl_2Si_2O_8$) doped with divalent as well as trivalent rare-earth ions show triboluminescence due to the $4f-4f$ and $4f-5d$ electronic transitions of the doped rare-earth ions. Akiyama *et al.*[17] found that intense triboluminescence takes place in polycrystalline $Sr_3Al_2O_6$:Eu,Dy. Xu *et al.*[18] demonstrated that $SrAl_2O_4:Eu^{2+}$ exhibits triboluminescence due to the $4f^7-4f^6 5d$ transition of Eu^{2+}. These phenomena are attracting considerable attention because they can be applied to sensing of structural damage and fracture.

The rare-earth-doped $SrAl_2O_4$ treated by Xu *et al.*[18] is known for its long lasting phosphorescence as well.[19] The long lasting phosphorescence is a phenomenon that a solid irradiated with UV or white light beforehand continues to emit light even after the excitation is ceased. In particular, $SrAl_2O_4$ doped with Eu^{2+} and Dy^{3+} shows intense phosphorescence with long lasting time. Although it was reported that the $SrAl_2O_4$ doped with Eu^{2+} exhibits triboluminescence as mentioned above, the atomistic depiction about the effect of stress or strain on the rare-earth ion still remains unclear. In the present investigation, we measured photoluminescence as well as triboluminescence spectra of Dy^{3+}-doped $(Sr,Ba)Al_2O_4$ and $(Sr,Ca)Al_2O_4$ polycrystals, and examined the difference between photoluminescence and triboluminescence for the purpose of evaluating the effect of fracture or deformation of crystal on the local structure and luminescence properties of doped rare-earth ions if such an effect is present. A choice of the Dy^{3+} comes from the fact that one can readily estimate the coordination state around Dy^{3+}, e.g., coordination symmetry and electronic state of chemical bond between Dy^{3+} and a ligand, on the basis of the relative intensity of emission lines caused by the $4f-4f$ transitions of Dy^{3+}.[20] In addition, using a solid solution such as $(Sr,Ba)Al_2O_4$ as the host material, one can vary the ligand field around Dy^{3+} systematically. As reported by Ito *et al.*,[21] there exist wide regions of solid solu-

a)Electronic mail: katsu@ipc.kit.ac.jp

TABLE I. Nominal composition (molar ratio) of Dy^{3+}-doped alkaline earth aluminate polycrystals prepared in the present study.

Nominal composition of samples	SrO	BaO	CaO	Al_2O_3	Dy_2O_3
$SrAl_2O_4:Dy^{3+}$	0.99			1.005	0.005
$Sr_{0.9}Ba_{0.1}Al_2O_4:Dy^{3+}$	0.895	0.095		1.005	0.005
$Sr_{0.8}Ba_{0.2}Al_2O_4:Dy^{3+}$	0.795	0.195		1.005	0.005
$Sr_{0.6}Ba_{0.4}Al_2O_4:Dy^{3+}$	0.595	0.395		1.005	0.005
$Sr_{0.9}Ca_{0.1}Al_2O_4:Dy^{3+}$	0.895		0.095	1.005	0.005
$Sr_{0.8}Ca_{0.2}Al_2O_4:Dy^{3+}$	0.795		0.195	1.005	0.005
$Sr_{0.6}Ca_{0.4}Al_2O_4:Dy^{3+}$	0.595		0.395	1.005	0.005

tion and the lattice parameter varies monotonically with composition in the $SrAl_2O_4$–$BaAl_2O_4$ and $SrAl_2O_4$–$CaAl_2O_4$ systems.

II. EXPERIMENTAL PROCEDURE

Polycrystalline $(Sr,Ba)Al_2O_4$ and $(Sr,Ca)Al_2O_4$ doped with Dy^{3+} were prepared from reagent-grade $SrCO_3$, $BaCO_3$, $CaCO_3$, Al_2O_3, and Dy_2O_3. These raw materials were weighed so that the nominal molar ratios listed in Table I were attained. The slight excess amount of Al compared with the stoichiometric composition, e.g., $SrAl_2O_4$ corresponds to the concentration of cation vacancy brought about by the replacement of the divalent alkaline earth ion with Dy^{3+} (trivalent cation). After the raw materials were mixed thoroughly, the mixture was calcined at 1100 °C for 5 h in air. The resultant powder was pressed under a hydrostatic pressure of 10 MPa, and sintered at 1600 °C for 3 h in air. The polycrystalline sample thus obtained was subjected to x-ray diffraction analysis with Cu $K\alpha$ radiation to identify crystalline phases.

The polycrystalline sample was pressed with a pressure device and triboluminescence spectrum was measured by using a charge-coupled-device detector (Hamamatsu Photonics, C5094) equipped with a multichannel analyzer (Hamamatsu Photonics, C5967). A uniaxial compressive stress was applied to the sample. The stress required for the fracture of the sample could not be estimated with our equipment. Measurements of photoluminescence spectra were carried out using a fluorescence spectrophotometer (Hitachi, 850). The excitation wavelength was 350 nm. Excitation spectra were measured by monitoring the emission at 572–574 nm. The measurements of triboluminescence, photoluminescence, and excitation spectra were performed at room temperature in air.

III. RESULTS

Figures 1 and 2 show x-ray diffraction patterns of the polycrystalline samples in $(Sr,Ca)Al_2O_4$ and $(Sr,Ba)Al_2O_4$ systems, respectively. As for the x-ray diffraction pattern of $SrAl_2O_4$ doped with Dy^{3+} shown at the lowest side in Figs. 1 and 2, almost all the diffraction lines are attributable to $SrAl_2O_4$ although very weak diffraction lines ascribed to $Dy_3Al_5O_{12}$ and $DyAlO_3$ are observed as indicated by the solid circle and triangles, respectively, in Figs. 1 and 2. A comparison of four diffraction patterns shown in Fig. 1 reveals that a drastic change of crystal structure takes place

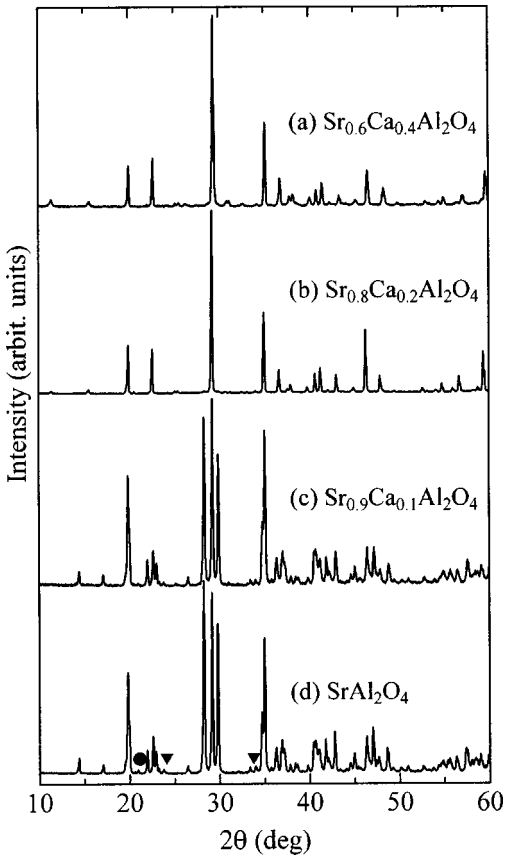

FIG. 1. X-ray diffraction patterns of Dy^{3+}-doped (a) $Sr_{0.6}Ca_{0.4}Al_2O_4$, (b) $Sr_{0.8}Ca_{0.2}Al_2O_4$, (c) $Sr_{0.9}Ca_{0.1}Al_2O_4$, and (d) $SrAl_2O_4$ polycrystals. Very weak diffraction lines indicated by closed circle and triangles are assigned to $Dy_3Al_5O_{12}$ and $DyAlO_3$, respectively.

when the composition is varied from $Sr_{0.9}Ca_{0.1}Al_2O_4$ to $Sr_{0.8}Ca_{0.2}Al_2O_4$, whereas the crystal structures of $SrAl_2O_4$ and $Sr_{0.9}Ca_{0.1}Al_2O_4$ are very similar to each other. Also, the x-ray diffraction pattern of $Sr_{0.6}Ca_{0.4}Al_2O_4$ is almost identical to that of $Sr_{0.8}Ca_{0.2}Al_2O_4$. A drastic change of crystal structure is, in particular, reflected by the intense diffraction lines at around $2\theta=28°–30°$; three intense diffraction lines are observed for $SrAl_2O_4$ and $Sr_{0.9}Ca_{0.1}Al_2O_4$, while only one intense line appears in the patterns of $Sr_{0.8}Ca_{0.2}Al_2O_4$ and $Sr_{0.6}Ca_{0.4}Al_2O_4$. In contrast, as shown in Fig. 2, the substitution of Sr by Ba in the $(Sr,Ba)Al_2O_4$ does not change the crystal structure so drastically. Even when 40% of Sr is replaced by Ba, the crystal structure still remains unchanged. According to the JCPDS cards (Nos. 31-1336 and 34-379), the x-ray diffraction patterns in Figs. 1 and 2 indicate that the crystal structure of $SrAl_2O_4$, $Sr_{0.9}Ca_{0.1}Al_2O_4$, and $Sr_{1-x}Ba_xAl_2O_4$ with $x=0.1$, 0.2, and 0.4, is mainly monoclinic, while the crystal structure of $Sr_{0.8}Ca_{0.2}Al_2O_4$ and $Sr_{0.6}Ca_{0.4}Al_2O_4$ is hexagonal.

Photoluminescence spectra are shown in Fig. 3 for polycrystalline $(Sr,Ba)Al_2O_4$ and $Sr_{0.9}Ca_{0.1}Al_2O_4$ doped with Dy^{3+}. The excitation was carried out at 350 nm. All the emission lines observed are ascribable to the $4f-4f$ transitions of Dy^{3+} as indicated in Fig. 3; the emission lines at around 480, 575, and 660 nm are assigned to the $^4F_{9/2}-^6H_{15/2}$, $^4F_{9/2}-^6H_{13/2}$, and $^4F_{9/2}-^6H_{11/2}$ transitions of

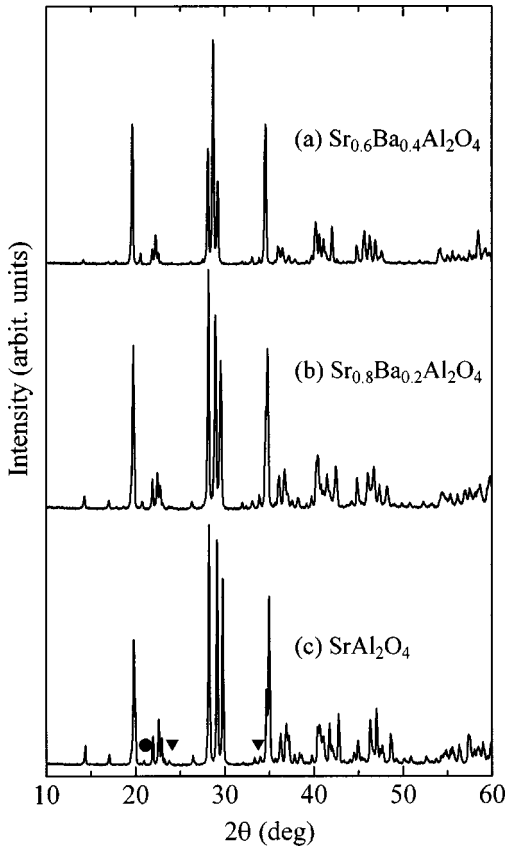

FIG. 2. X-ray diffraction patterns of Dy^{3+}-doped (a) $Sr_{0.6}Ba_{0.4}Al_2O_4$, (b) $Sr_{0.8}Ba_{0.2}Al_2O_4$, and (c) $SrAl_2O_4$ polycrystals. Very weak diffraction lines indicated by closed circle and triangles are assigned to $Dy_3Al_5O_{12}$ and $DyAlO_3$, respectively.

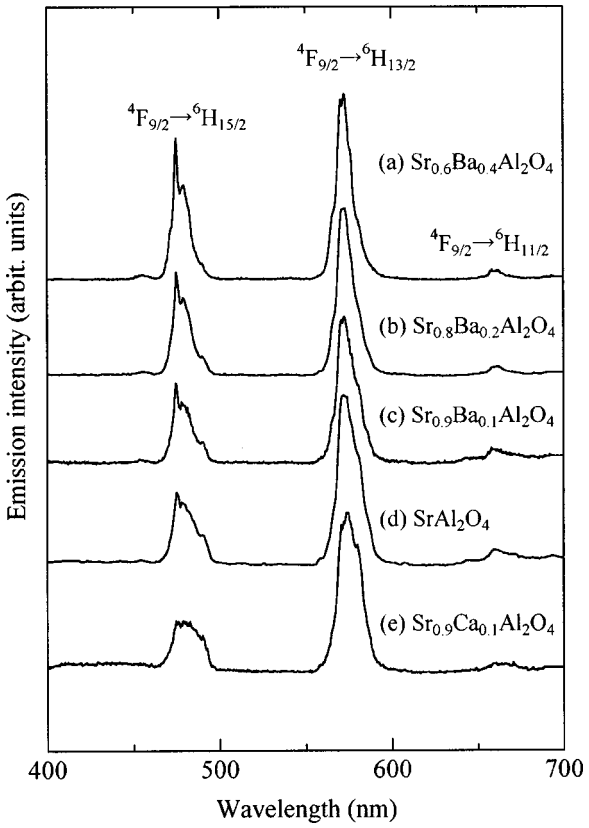

FIG. 3. Photoluminescence spectra of Dy^{3+}-doped (a) $Sr_{0.6}Ba_{0.4}Al_2O_4$, (b) $Sr_{0.8}Ba_{0.2}Al_2O_4$, (c) $Sr_{0.9}Ba_{0.1}Al_2O_4$, (d) $SrAl_2O_4$, and (e) $Sr_{0.9}Ca_{0.1}Al_2O_4$. The excitation wavelength is 350 nm. The emission lines are assigned to the $4f-4f$ transitions of Dy^{3+}, as indicated in the figure.

Dy^{3+}, respectively. It is found in Fig. 3 that the relative intensity of the 480 nm emission compared with the 575 nm emission varies with composition; the relative intensity of emission line at 480 nm increases monotonically with the substitution of Sr by Ba. In Fig. 4 are shown triboluminescence spectra of $(Sr,Ba)Al_2O_4$ and $Sr_{0.9}Ca_{0.1}Al_2O_4$ doped with Dy^{3+}. The emission lines due to the $^4F_{9/2}-{}^6H_{15/2}$, $^4F_{9/2}-{}^6H_{13/2}$, and $^4F_{9/2}-{}^6H_{11/2}$ transitions of Dy^{3+} are observed. A comparison between Figs. 3 and 4 reveals that the compositional dependence of intensity ratio of 480 to 575 nm emission is different between photoluminescence and triboluminescence. In other words, the intensity ratio of the 480 to 575 nm emission is almost independent of the composition in the triboluminescence spectra, whereas the relative intensity of the 480 nm emission changes with composition in the photoluminescence as mentioned above. In addition, it seems that the intensity ratio of the 480 to 575 nm emission is smaller in the triboluminescence spectra than in the photoluminescence spectra. These phenomena are discussed below.

Figure 5 shows photoluminescence spectra of $SrAl_2O_4$, $Sr_{0.8}Ca_{0.2}Al_2O_4$, and $Sr_{0.6}Ca_{0.4}Al_2O_4$ doped with Dy^{3+}. The excitation was carried out at 350 nm. As for the emission line at 480 nm, the profile for $Sr_{0.8}Ca_{0.2}Al_2O_4:Dy^{3+}$ is almost identical to that for $Sr_{0.6}Ca_{0.4}Al_2O_4:Dy^{3+}$, while $SrAl_2O_4:Dy^{3+}$ manifests an appearance different from the other two crystals. In addition, the emission line at 575 nm for $SrAl_2O_4:Dy^{3+}$ is somewhat shifted to a shorter-wavelength side compared with the other two crystals. The difference in photoluminescence spectra between $SrAl_2O_4:Dy^{3+}$ and $Sr_{1-y}Ca_yAl_2O_4:Dy^{3+}$ with $y=0.2$ and 0.4 is coincident with the discrepancy in crystal structure indicated in Fig. 1. Furthermore, it should be noted that triboluminescence was barely observed in $Sr_{0.8}Ca_{0.2}Al_2O_4:Dy^{3+}$ and $Sr_{0.6}Ca_{0.4}Al_2O_4:Dy^{3+}$.

IV. DISCUSSION

As mentioned above, the intensity ratio of the 480 to 575 nm emission is smaller in the triboluminescence spectra than in the photoluminescence spectra for $(Sr,Ba)Al_2O_4:Dy^{3+}$ and $Sr_{0.9}Ca_{0.1}Al_2O_4:Dy^{3+}$. One possible origin for this phenomenon is the self-absorption. In other words, because the photons are emitted from the rare-earth ions within the bulk sample in the case of triboluminescence, some of the photons are readily reabsorbed by the other rare-earth ions until the photons come out of the sample. In contrast, the photoluminescence is measured only for the rare-earth ion suited near the surface of the sample, so that the self-absorption cannot take place. For instance, it is clear that the self-absorption is a cause for the difference in triboluminescence and photoluminescence spectra at a short-wavelength range (400–500 nm or so) for $BaAl_2Si_2O_8:Eu^{2+}$.[22] In order to ascertain whether or not the smaller relative emission intensity at 480 nm in the triboluminescence spectra is attributable to the

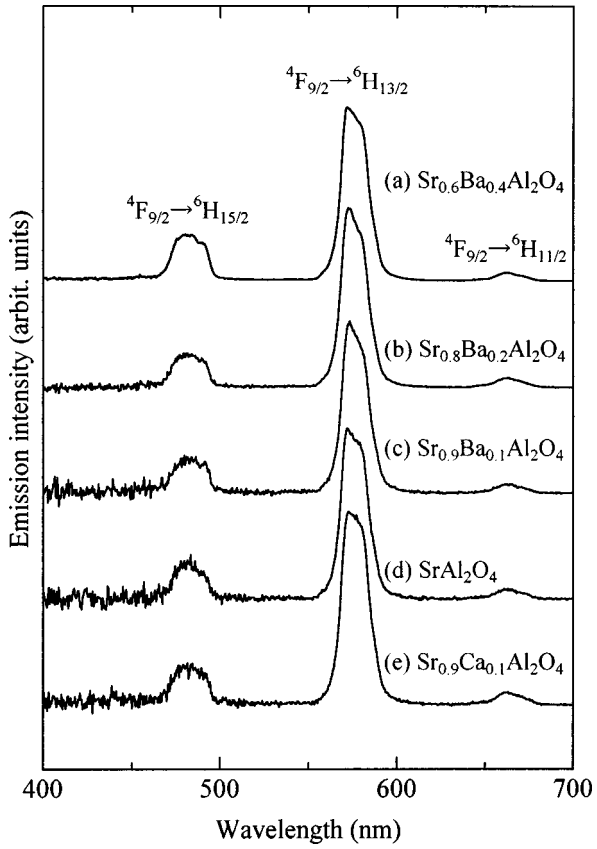

FIG. 4. Triboluminescence spectra of Dy^{3+}-doped (a) $Sr_{0.6}Ba_{0.4}Al_2O_4$, (b) $Sr_{0.8}Ba_{0.2}Al_2O_4$, (c) $Sr_{0.9}Ba_{0.1}Al_2O_4$, (d) $SrAl_2O_4$, and (e) $Sr_{0.9}Ca_{0.1}Al_2O_4$. The emission lines are assigned to the $4f-4f$ transitions of Dy^{3+}, as indicated in the figure.

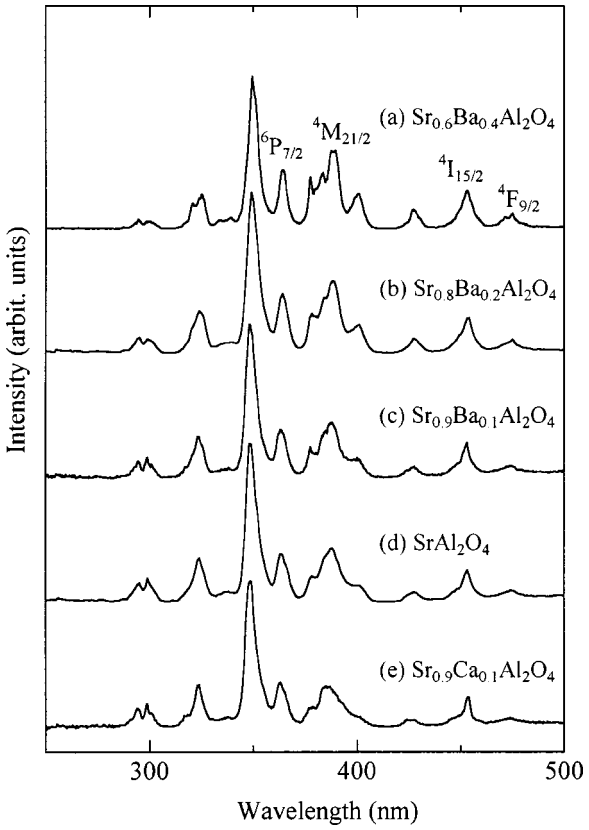

FIG. 6. Excitation spectra of Dy^{3+}-doped (a) $Sr_{0.6}Ba_{0.4}Al_2O_4$, (b) $Sr_{0.8}Ba_{0.2}Al_2O_4$, (c) $Sr_{0.9}Ba_{0.1}Al_2O_4$, (d) $SrAl_2O_4$, and (e) $Sr_{0.9}Ca_{0.1}Al_2O_4$.

self-absorption, we carried out measurements of excitation spectra. The results are shown in Fig. 6. An absorption band due to the $^6H_{15/2}-{}^4F_{9/2}$ transition is observed at around 475 nm, although the intensity is weak compared with other lines. Figure 7 shows emission or absorption line at around 480 nm ($^6H_{15/2}-{}^4F_{9/2}$ transition) in triboluminescence (closed circles), photoluminescence (solid line), and excitation (open circles) spectra of $SrAl_2O_4$:Dy^{3+}. It is found that an overlap of photoluminescence and excitation spectra is present at around 475 nm. However, it is difficult to compare quantitatively the intensity of these emission and absorption lines because the accurate number of photons emitted or absorbed was not obtained in the measurements. Hence, at this

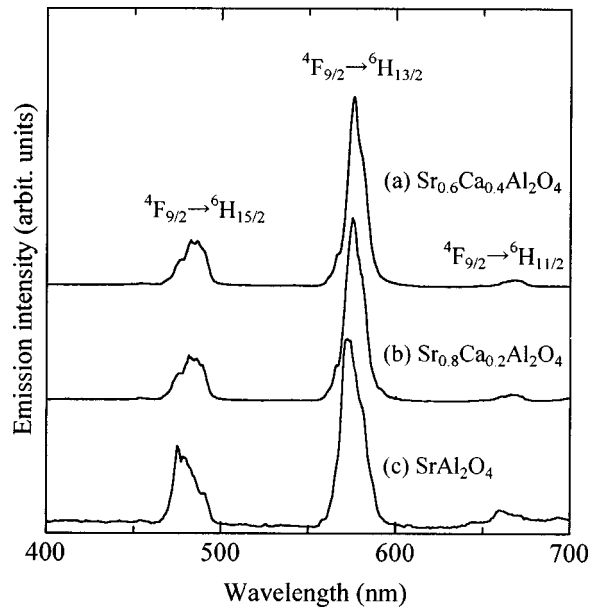

FIG. 5. Photoluminescence spectra of Dy^{3+}-doped (a) $Sr_{0.6}Ca_{0.4}Al_2O_4$, (b) $Sr_{0.8}Ca_{0.2}Al_2O_4$, and (c) $SrAl_2O_4$. The excitation wavelength is 350 nm.

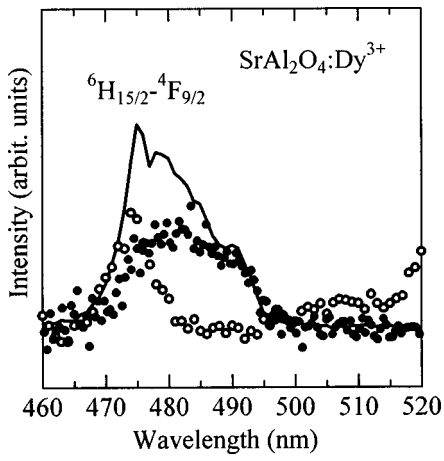

FIG. 7. Triboluminescence (closed circles), photoluminescence (solid line), and excitation (open circles) spectra of $SrAl_2O_4$:Dy^{3+}. Emission or absorption line at around 480 nm, which is brought about by the $^6H_{15/2}-{}^4F_{9/2}$ transition of Dy^{3+}, is shown.

moment, we cannot rule out the possibility of self-absorption, which can cause the smaller relative emission intensity at 480 nm in the triboluminescence spectra, although the degree of contribution by the self-absorption is thought to be small, as discussed below.

Another possibility is the effect of the ligand field around Dy^{3+} on the emission intensity. It is known that the radiative transition probability among the $4f$ levels in a rare-earth ion is closely related to the characteristics of the ligand field around the rare-earth ion. According to Judd–Ofelt theory,[23,24] the line strength $S(aJ:bJ')$ corresponding to the electric dipole transition between $|a\rangle$ and $|b\rangle$ states is expressed as follows:

$$S(aJ:bJ')=\sum_{t=2,4,6}\Omega_t|\langle aJ\|U^{(t)}\|bJ'\rangle|^2, \quad (1)$$

where J and J' denote the total angular momentum, and $\langle aJ\|U^{(t)}\|bJ'\rangle$ and Ω_t are called the reduced matrix element and Ω parameter, respectively. The reduced matrix element can be calculated for each electronic transition of rare-earth ions. On the other hand, the Ω parameter is dependent on the ligand field around a rare-earth ion. Thus, since the line strength is proportional to the integrated intensity of lines in optical absorption and emission spectra, the Ω parameter corresponding to the characteristics of the ligand field is reflected by the integrated intensity of absorption and emission lines. The physical meaning of Ω parameters has been argued by many researchers. It is thought that Ω_2 reflects the coordination symmetry of ligands and Ω_6 is related to the covalency of the chemical bond between a rare-earth ion and a ligand.[25,26]

As for the Dy^{3+}, the integrated intensity ratio of 480 to 575 nm emission correlates with Ω_6/Ω_2, suggesting that the integrated emission intensity ratio becomes small when the coordination symmetry for Dy^{3+} is low.[20] We evaluated the integrated intensity ratio $I(480\,\text{nm})/I(575\,\text{nm})$ for the present polycrystalline samples on the basis of the triboluminescence and photoluminescence spectra in Figs. 3 and 4. The results are shown in Fig. 8. In Fig. 8, the mean ionic radius of alkaline earth in the crystals is plotted as the abscissa. In calculation of the mean ionic radius, the values of ionic radii proposed by Shannon[27] for 12-coordinated alkaline earth ions were adopted because the coordination number for Ba^{2+} in hexagonal $BaAl_2O_4$ was reported to be 12,[28] and the molar fraction of alkaline earth ions in the crystals was simply taken into account. In Fig. 8, open and closed circles represent triboluminescence and photoluminescence, respectively. Two features are found in Fig. 8. First, $I(480\,\text{nm})/I(575\,\text{nm})$ increases monotonically with an increase in the mean ionic radius in the case of photoluminescence, whereas $I(480\,\text{nm})/I(575\,\text{nm})$ is almost independent of the mean ionic radius for the triboluminescence. Second, the values of $I(480\,\text{nm})/I(575\,\text{nm})$ for the triboluminescence are smaller than those for the photoluminescence. According to the above argument, the tendency observed for the photoluminescence reflects the variation of the ligand field around Dy^{3+} with the composition of crystal. Namely, the luminescence centers, i.e., Dy^{3+} ions, with different atomic configurations or ligand fields, are formed depending on the composition. In contrast, the behavior of $I(480\,\text{nm})/I(575\,\text{nm})$ observed for the triboluminescence indicates that the coordination symmetry for Dy^{3+}, which brings about the triboluminescence, is independent of the kinds of crystals. In addition, the small value of $I(480\,\text{nm})/I(575\,\text{nm})$ in triboluminescence spectra suggests that the coordination symmetry for Dy^{3+}, which contributes to the triboluminescence, is low. These results lead to speculation that the emission of photons from Dy^{3+} placed in a distorted site, such as a fractured surface and/or the vicinity of a crack tip, is observed as the triboluminescence irrespective of the kinds of crystals.

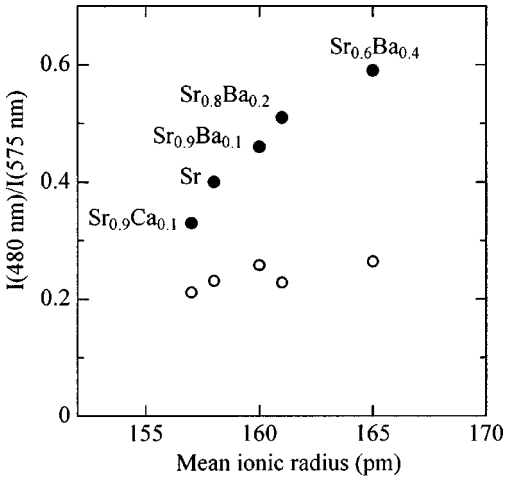

FIG. 8. Integrated emission intensity ratio, $I(480\,\text{nm})/I(575\,\text{nm})$, as a function of mean ionic radius of alkaline earth in the crystals. Open and closed circles correspond to the triboluminescence and photoluminescence, respectively.

Figure 9 indicates a direct comparison of the 575 nm emission line ($^4F_{9/2}-^6H_{13/2}$ transition) between triboluminescence (closed circles) and photoluminescence (solid line) of $SrAl_2O_4:Dy^{3+}$. This emission line is composed of two components at least due to the splitting of energy levels

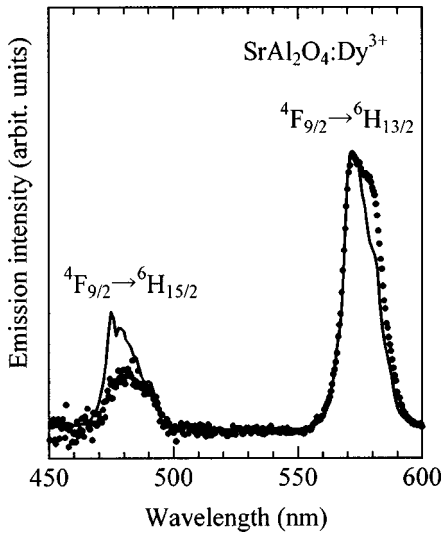

FIG. 9. Comparison of 575 nm emission line ($^4F_{9/2}-^6H_{13/2}$ transition) between triboluminescence (closed circles) and photoluminescence (solid line) spectra of $SrAl_2O_4:Dy^{3+}$.

caused by the crystal field, and the relative intensity of one component at the longer-wavelength side is larger in the triboluminescence spectrum than in the photoluminescence spectrum. Similar phenomena are observed for other samples, as shown in Figs. 3 and 4. It is clear that this difference cannot be attributed to self-absorption because there is no absorption band at around 575 nm considering the electronic levels of Dy^{3+}. Qualitatively speaking, this difference in relative emission intensity reflects a difference in crystal field, and hence, the result shown in Fig. 9 supports that the state of the ligand field around the Dy^{3+}, which gives rise to the triboluminescence, is different from that relevant to the photoluminescence, i.e., the second possibility described above. Thus, the difference in the ligand field is presumably the main reason and the self-absorption mentioned above is the minor reason for the difference between triboluminescence and photoluminescence spectra.

The fact that $SrAl_2O_4$, $Sr_{0.9}Ca_{0.1}Al_2O_4$, and $Sr_{1-x}Ba_xAl_2O_4$ with $x=0.1$, 0.2, and 0.4 doped with Dy^{3+} exhibit intense triboluminescence, although the triboluminescence is barely observed for $Sr_{0.8}Ca_{0.2}Al_2O_4$:Dy^{3+} and $Sr_{0.6}Ca_{0.4}Al_2O_4$:Dy^{3+}, is presumably attributable to the difference in crystal structure. Chandra[29] summarized the relationship between crystal structure and triboluminescence. According to him, the symmetry of the crystal structure, which allows piezoelectricity, gives rise to the triboluminescence, and vice versa. However, there is an exception; as reported previously, $BaAl_2Si_2O_8$ shows intense triboluminescence although it has a $D_{6h}(P6/mmm)$ symmetry which precludes piezoelectricity. According to Hanic, Chemekova, and Majling,[30] the space group of monoclinic $SrAl_2O_4$, is $P2_1$ or $P2_1/m$, and the hexagonal $SrAl_2O_4$ has a space group of $P6_322$ (JCPDS cards No. 31-1336). Since the symmetry of the crystal structure of monoclinic $SrAl_2O_4$ is not clarified, it is difficult to discuss the occurrence of triboluminescence in connection with the crystal structure of the $SrAl_2O_4$ phase at this moment. Therefore, the process of excitation of Dy^{3+} in the triboluminescence still remains unclear. One possible mechanism is a discharge at the fractured surface. Some charged species, such as an electron emitted from the fractured surface, may directly excite the Dy^{3+} ion in the vicinity of the fractured surface. Also, it is possible that the charged particles excite the molecules in air, such as N_2, to bring about emission of photons, which excite the Dy^{3+} ions. Further investigation is required for thorough clarification of triboluminescence in Dy^{3+}-doped alkaline earth aluminates.

V. CONCLUSIONS

Measurements of triboluminescence and photoluminescence for polycrystalline $(Sr,Ba)Al_2O_4$ and $(Sr,Ca)Al_2O_4$ doped with Dy^{3+} were carried out. Although all the crystals examined in the present study exhibit photoluminescence due to the $4f-4f$ transitions of Dy^{3+}, the triboluminescence, which was caused by the $4f-4f$ transitions of Dy^{3+} as well, took place only in $Sr_{1-x}Ba_xAl_2O_4$:Dy^{3+} with $x=0$, 0.1, 0.2, and 0.4 and $Sr_{0.9}Ca_{0.1}Al_2O_4$:Dy^{3+}; triboluminescence was barely observed in $Sr_{0.8}Ca_{0.2}Al_2O_4$:Dy^{3+} and $Sr_{0.6}Ca_{0.4}Al_2O_4$:Dy^{3+}. This phenomenon is presumably ascribable to the difference in crystal structure among these compounds.

The dependence of relative emission intensity on the composition of crystal observed in the triboluminescence spectra is different from that in the photoluminescence spectra. Two possible origins are proposed for this phenomenon. One of them is the self-absorption due to Dy^{3+}, which may take place in the triboluminescence. The other is the situation that the $4f-4f$ transitions of Dy^{3+} placed in a distorted site, such as a fractured surface and/or the vicinity of a crack tip, brings about the triboluminescence. We speculate that the latter is the main reason for the difference between triboluminescence and photoluminescence spectra.

[1] A. J. Walton, Adv. Phys. **26**, 887 (1977).
[2] L. M. Belyaev and Yu. N. Martyshev, Phys. Status Solidi **34**, 57 (1969).
[3] L. Sodomka, Phys. Status Solidi A **7**, K65 (1971).
[4] J. I. Zink, Chem. Phys. Lett. **32**, 236 (1975).
[5] G. P. Williams, Jr. and T. J. Turner, Solid State Commun. **29**, 201 (1979).
[6] B. P. Chandra and J. I. Zink, J. Chem. Phys. **73**, 5933 (1980).
[7] J. I. Zink, W. Beese, and J. W. Schindler, Appl. Phys. Lett. **40**, 112 (1982).
[8] G. N. Chapman and A. J. Walton, J. Appl. Phys. **54**, 5961 (1983).
[9] R. Nowak, A. Krajewska, and M. Samoc, Chem. Phys. Lett. **94**, 270 (1983).
[10] B. T. Brady and G. A. Rowell, Nature (London) **321**, 488 (1986).
[11] K. Nakayama, N. Suzuki, and H. Hashimoto, J. Phys. D **25**, 303 (1992).
[12] D. G. Li, N. S. McAlpine, and D. Haneman, Surf. Sci. **281**, L315 (1993).
[13] Y. Kawaguchi, Jpn. J. Appl. Phys., Part 1 **37**, 1892 (1998).
[14] G. N. Chapman and A. J. Walton, J. Phys. C **16**, 5543 (1983).
[15] T. Ishihara, K. Tanaka, K. Hirao, and N. Soga, Jpn. J. Appl. Phys., Part 2 **36**, L781 (1997).
[16] T. Ishihara, K. Tanaka, K. Fujita, K. Hirao, and N. Soga, Solid State Commun. **107**, 763 (1998).
[17] M. Akiyama, C.-N. Xu, K. Nonaka, and T. Watanabe, Appl. Phys. Lett. **73**, 3046 (1998).
[18] C.-N. Xu, T. Watanabe, M. Akiyama, and X.-G. Zheng, Appl. Phys. Lett. **74**, 2414 (1999).
[19] T. Matsuzawa, Y. Aoki, N. Takeuchi, and Y. Murayama, J. Electrochem. Soc. **143**, 2670 (1996).
[20] S. Tanabe, T. Hanada, M. Watanabe, T. Hayashi, and N. Soga, J. Am. Ceram. Soc. **78**, 2917 (1995).
[21] S. Ito, S. Banno, K. Suzuki, and M. Inagaki, J. Ceram. Soc. Jpn. **87**, 344 (1979).
[22] J. P. Duignan, I. D. H. Oswald, I. C. Sage, L. M. Sweeting, K. Tanaka, T. Ishihara, K. Hirao, and G. Bourhill (unpublished).
[23] B. R. Judd, Phys. Rev. **127**, 750 (1962).
[24] G. S. Ofelt, J. Chem. Phys. **37**, 511 (1962).
[25] S. Tanabe, T. Ohyagi, N. Soga, and T. Hanada, Phys. Rev. B **46**, 3305 (1992).
[26] S. Tanabe, T. Ohyagi, S. Todoroki, T. Hanada, and N. Soga, J. Appl. Phys. **73**, 8451 (1993).
[27] R. D. Shannon, Acta Crystallogr., Sect. A: Cryst. Phys., Diffr., Theor. Gen. Crystallogr. **32**, 751 (1976).
[28] M. Nayak and T. R. N. Kutty, Mater. Res. Bull. **31**, 227 (1996).
[29] B. P. Chandra, Nucl. Tracks Radiat. Meas. **10**, 225 (1985).
[30] F. Hanic, T. Yu. Chemekova, and J. Majling, J. Appl. Crystallogr. **12**, 243 (1979).